Available online at www.sciencedirect.com
ScienceDirect
Journal of Bionic Engineering 13 (2016) 572–584

Adaptive Walking Control of Biped Robots Using Online Trajectory Generation Method Based on Neural Oscillators

Chengju Liu[1], Danwei Wang[2], Erik David Goodman[3], Qijun Chen[1]

1. *School of Electronics and Information Engineering*, *Tongji University*, *Shanghai* 201804, *China*
2. *School of Electrical and Electronic Engineering*, *Nanyang Technological University*, *Manyang Avenue* 639798, *Singapore*
3. *BEACON Center for the Study of Evolution in Action*, *Michigan State University*, *East Lansing* 48824, *USA*

Abstract

This work concerns biped adaptive walking control on irregular terrains with online trajectory generation. A new trajectory generation method is proposed based on two neural networks. One oscillatory network is designed to generate foot trajectory, and another set of neural oscillators can generate the trajectory of Center of Mass (CoM) online. Using a motion engine, the characteristics of the workspace are mapped to the joint space. The entraining property of the neural oscillators is exploited for adaptive walking in the absence of a priori knowledge of walking conditions. Sensory feedback is applied to modify the generated trajectories online to improve the walking quality. Furthermore, a staged evolutionary algorithm is developed to tune system parameters to improve walking performance. The developed control strategy is tested using a humanoid robot on irregular terrains. The experiments verify the success of the presented strategy. The biped robot can walk on irregular terrains with varying slopes, unknown bumps and stairs through autonomous adjustment of its walking patterns.

Keywords: biped robot, adaptive walking, neural oscillator, trajectory generation, staged evolution algorithm

doi: 10.1016/S1672-6529(16)60329-3

1 Introduction

Biped locomotion control is fundamental for biped robots to work in unknown walking conditions. Many biped robots successfully utilize Zero Moment Point (ZMP) based locomotion control methods[1–6]. Most researches focus on walking stability of biped robots on flat terrain or on known uneven terrains. The trajectory-based methods are good for a robot to walk according to pre-designed trajectories while maintaining its balance. However, pre-designed trajectories are fixed and therefore, if terrain conditions change, pre-designed trajectories may fail. Although multiple trajectories for different terrains can be designed, and switching is possible while walking, they cannot cover all situations a robot might encounter.

For a biped robot walking on different terrains, like overcoming obstacle[7], it is necessary to adapt to walking terrains with adjustable workspace trajectories. As the complexity of walking conditions increases, the polynomial interpolation method becomes inefficient. The polynomial order becomes too high and its computation will be too demanding. To overcome this problem, Shih[1] proposed a strategy that uses cubic spline interpolation to plan foot trajectories. Huang *et al*.[2] formulated the constraints of foot motion parameters to produce different types of foot motion for various terrains. Park *et al*.[5] presented a gait trajectory generation method based on the combination of sinusoidal functions and 3rd-order polynomial functions to realize free gait biped walking. Based on ZMP, a gait synthesis technique was employed by Seven *et al*.[6]. The pitch angle reference for the foot sole plane was modified in real time using a fuzzy logic system to adapt to various walking slopes.

Human walking does not exhibit the characteristics of precise trajectory tracking. Biological researches show that the human walking is the consequence of the combination of inherent patterns and reflexes[8,9]. Researchers investigated bio-inspired control methods based on biomechanics of musculoskeletal system and motor neural networks[10,11]. Inspired by Central Pattern

Corresponding author: Qijun Chen
E-mail: qjchen@tongji.edu.cn

Generator (CPG), locomotion control methods have been proved workable[12–15]. CPG is a type of oscillator network that can produce rhythmic oscillatory signals endogenously. Through mutual inhibition of the neurons and entrainment with sensory feedback, the movement patterns of the network can be adjusted. The CPG-based motion control methods have been successfully used in swinging and crawling robots[16,17], as well as multi-legged robots[18,19]. For the control of biped locomotion[20–23], inspired by Taga's work[24,25], the walking control strategies are exploring in recent years.

The CPG-inspired motion control strategies are usually synthesized into joint-space control method and workspace control method. For the joint-space control methods, usually using one CPG unit to control one Degree of Freedom (DoF) of the robot, and the distributed oscillator network can generate complex coordinated multi-dimensional signals used as force or torque control to realize the coordinated motion. Due to the inherent instability of biped walking, the traditional joint space CPG control methods are not very feasible. For biped walking control, CPGs are usually used as supplements to other controllers.

For legged animals, the tips of the legs reflect gait patterns. Task space based study of animal walking mechanism can be an efficient way for CPG-inspired walking control of legged robots. Endo *et al*. [26], Ha *et al*.[27] and Aoi *et al*.[28] designed motion control strategies in the workspace space of biped robots. By using nonlinear oscillators to generate the nominal trajectories of the joints and the nominal trajectories are modified using feedback information that depend on the posture and motion of the biped robot to achieve robust walking[28]. To further develop the biped environmental adaptive walking capability, an online trajectory generation method should improve the dynamic stability and adaptability of any robot. That is, the generated trajectories should be modulated online according to the terrain conditions. In our previous work[29], using nonlinear oscillators, a CoM trajectory generator and a workspace trajectory modulator are designed. However, the pre-designed fixed foot trajectory limits the environmental adaptability. This paper aims to improve the walking adaptability on irregular terrain using neural oscillators. The adaptive foot trajectory and robust CoM trajectory can be generated online. In this paper, the following contributions are achieved:

(1) A new workspace trajectory generation method is presented based on a neural network consisted of four coupled nonlinear oscillators. The output signals of the neural network are transformed into the workspace trajectories for the two legs of a biped robot;

(2) A staged process is designed to evolve the parameters of the control system offline (using Webots platform). Firstly, numerical simulation is employed to analyze the effect of each parameter on the oscillatory output. Then, an NSGA-based method is used to realize the walking pattern evolution;

(3) Through the entrainment of the oscillators and the feedback signals of the biped robot, the generated CoM and foot trajectories can be modulated online according to the walking conditions to realize adaptive walking.

The motion engine will be used to realize the mapping from workspace to joint space (Ref. [30]). Thus, the adaptive joint control signals can drive all leg joints to realize the desired motion. The advantages of this proposed method are that it does not require prior information on the terrain conditions, nor does it rely on range sensor information for surface topology measurement. Both Webots simulations and real experiments are designed to demonstrate the efficiency of the presented control system. The rest of this paper is organized as follows: Section **2** introduces the design methods of the trajectory generators, the feedback path design and the parameter evolution of the control system. Section **3** describes the humanoid robot NAO and presents the simulation and experimental results of the various irregular terrain adaptive walking. The conclusion and discussion of this work and the future work are stated in Sections **4**.

2 Control system

For a biped robot to realize adaptive walking, the swing foot trajectory needs to be adjusted online to realize various walking patterns. In order to best improve the stability and adaptability, the modulation of swing foot trajectory and CoM trajectory should be combined. In the following sections, the trajectory generation methods are presented.

2.1 CPG-based trajectory generators

2.1.1 CPG model

A neural oscillator model evolved from

Refs. [19,31] is used as the CPG model as:

$$\begin{aligned} T_r \dot{u}_i^{\{e,f\}} &= -u_i^{\{e,f\}} - w_{fe} r_i^{\{f,e\}} - \beta v_i^{\{e,f\}} \\ &\quad + \sum_{j=1}^{n} w_{ij} r_j^{\{e,f\}} + s_0 + feed_i^{\{e,f\}}, \\ T_a \dot{v}_i^{\{e,f\}} &= -v_i^{\{e,f\}} + r_i^{\{e,f\}}, \\ r_i^{\{e,f\}} &= \max(u_i^{\{e,f\}}, 0), \\ r_i &= u_i^{\{f\}} - u_i^{\{e\}}, \end{aligned} \tag{1}$$

where the subscripts i, e and f denote the ith oscillator, an Extensor Neuron (EN) and a Flexor Neuron (FN), respectively. u_i is the inner state, v_i represents the degree of the self-inhibition effect; Parameters T_r and T_a are time constants; w_{fe} is the connecting weight between FN and EN; w_{ij} is the weight of the inhibitory synaptic connection between the ith and jth neurons; β represents the degree of the self-inhibition influence on the inner states u_i, s_0 is the external input. $Feed_i^{\{e,f\}}$ represents the sensory feedback.

2.1.2 Foot trajectory generator

The structure of the proposed swing foot trajectory generator is shown in Fig. 1, which is composed of a CPG network and a transform function. The transform function is designed to map the oscillatory outputs with specific phase relationships to the positions of the toes of the biped robot.

Using the proposed foot trajectory generator, the swing foot trajectories of the two legs can be generated in real time. The oscillatory networks are very suited to integrate sensory feedback signals, so when entrained with the feedback information from the robot and environment interaction, the expected adaptive foot trajectories can be generated.

It is known that swing movements in the x-direction (forward) and z-direction (vertical) for the same leg need a phase difference of π/2. For bipedal systems, the positions of both legs along z direction and x direction differ symmetrically with a phase difference of π. If the connection weights between oscillators are designed as inhibitory connections, the phase difference between F_x^{r} (F_x^{l}) and F_z^{r} (F_z^{l}) can be obtained as π/2, and the phase difference between F_x^{r} (F_z^{r}) and F_x^{l} (F_z^{l}) can be realized as π. In this study, the weights $\boldsymbol{W}_{ij} = (w_{ij})_{4\times4}$, inhibitory connections, are set as $w_{ij} = -1$ ($i \neq j$). Oscillation signals with specific phase differences required can be obtained

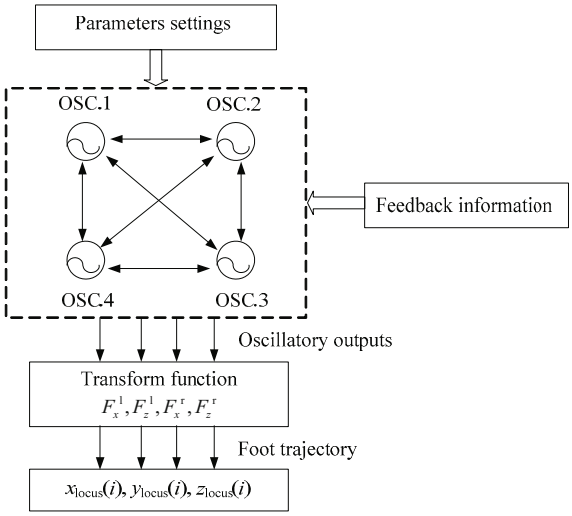

Fig. 1 The structure of the foot trajectory generator.

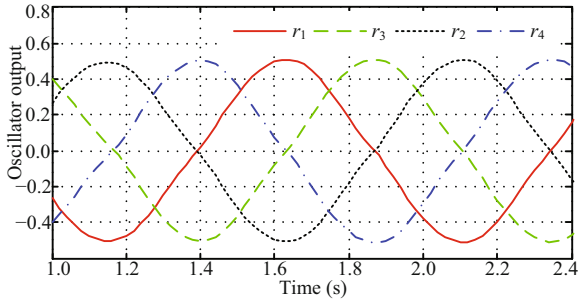

Fig. 2 The generated oscillatory outputs (where $T_r = 0.2$, $T_a = 0.4$, $s_0 = 0.6$, $\beta = 3.5$, $w_{fe} = 2.0$).

as shown in Fig. 2.

The transform functions are proposed to map the oscillatory outputs with amplitude transitions to the swing foot trajectories for two legs. The mapping processes only consider the positive part of the oscillation signals as follows

The mapping function for the left leg:

$$\left.\begin{aligned} F_x^{l} &= x_0 + A_x r_2 \\ F_z^{l} &= z_0 + A_z r_4 \end{aligned}\right\}, \tag{2}$$

where r_2 and r_4 are the output signals of oscillator-2 and oscillator-4 as shown in Fig. 1. Therefore, F_x^{l} and F_z^{l} have a π/2 phase difference. Parameters A_x and A_z are the amplitude scaling factors and parameters x_0 and z_0 are the foot position offsets.

The mapping function for the right leg:

$$\left.\begin{aligned} F_x^{r} &= x_0 + A_x r_1 \\ F_z^{r} &= z_0 + A_z r_3 \end{aligned}\right\}, \tag{3}$$

where r_1 and r_3 are the output signals of oscillator-1 and

oscillator-3, so F_x^{r} and F_z^{r} have a π/2 phase difference. The phase difference between F_x^{l} (F_z^{l}) and F_x^{r} (F_z^{r}) is the same phase relationship as that between r_2 (r_4) and r_1 (r_3), namely, π.

Due to the dynamic properties of the neural oscillators, modulation of the oscillator model parameters allows easy adjustment of the cycle period and the amplitude of the outputs. Here, the various biped walking patterns can be realized. This is a critical step to realize adaptive walking robust to various environment.

2.1.3 CoM trajectory generator

Three neural oscillators are used to generate three dimensional components of a CoM trajectory as:

$$\left.\begin{aligned} \mathrm{CoM}_x &= offset_x + K_{\mathrm{CoM}x} r_{1\_\mathrm{CoM}} + K_f t \\ \mathrm{CoM}_y &= offset_y + K_{\mathrm{CoM}y} r_{2\_\mathrm{CoM}} \\ \mathrm{CoM}_z &= offset_z + K_{\mathrm{CoM}z} r_{3\_\mathrm{CoM}} \end{aligned}\right\}, \tag{4}$$

where $offset_x$, $offset_y$ and $offset_z$ are position offsets, parameters K_x, K_y, K_z and K_f are the gain coefficients, r_{1_CoM}, r_{2_CoM} and r_{3_CoM} are output signals of the neural oscillators. By Modulated the adjustable parameters in Eq. (4) can generate robust CoM trajectory.

2.2 Improvement of stability and adaptability

Entrainment with the sensory feedback information is a good way to improve the adaptability of the robot walking[32–35]. In this work, as Fig. 3 shows, the body attitude information and ZMP information are used as feedback information to modulate the generated trajectories online to improve the walking quality.

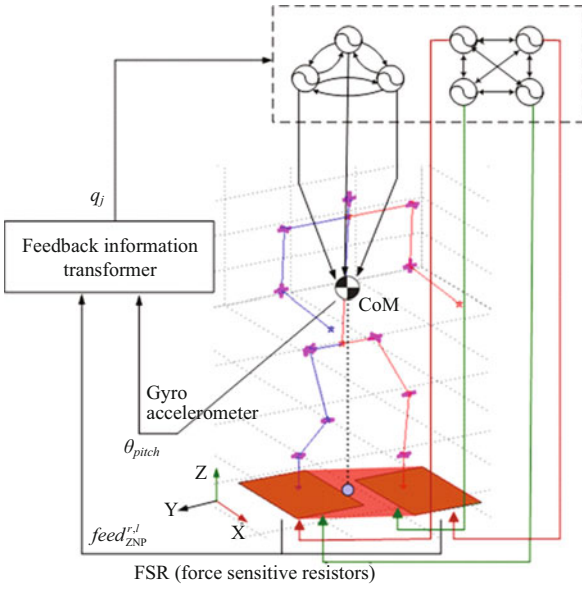

Fig. 3 The structure of feedback loop.

2.2.1 Body-attitude-based feedback path

In this work, the body attitude angle θ_{pitch} is applied to automatically modulate the generated swing foot trajectory and CoM trajectory to mimic this reflex, to adjust the position of the tip of legs and the position of the CoM according to the walking condition. The sensory feedback loop is designed as:

$$feed_{\mathrm{VSR}} = K_{\mathrm{VSR}} \times \theta_{\mathrm{pitch}}, \tag{5}$$

where K_{VSR} is the gain coefficient.

2.2.2 ZMP-based feedback

This work wants to modulate in real time the outputs of the oscillators corresponding to the foot trajectories in coupling with the ZMP feedback. The distance between the ZMP and the sole edge is an important indicator of stability in walking. The ZMP should be kept as far from the boundary as possible to counter unexpected perturbations from environment (in this work, the measured variable is the Center of Pressure (CoP)), so the feedback path can be formulated as:

$$feed_{\mathrm{ZMP}}^{\{\mathrm{e,f}\}} = K_{\mathrm{ZMP}} \times D_s, \tag{6}$$

where K_{ZMP} is the gain coefficient, and D_{s} is the stability margin, namely, the smaller value of $D_{sx} = \mathrm{ZMP}_x - S_x$ and $D_{sy} = \mathrm{ZMP}_y - S_y$ (S_x and S_y are x and y positions of the sole edges).

2.3 Staged system parameters evolution

As there is no proven methodology for CPG parameter tuning, two main alternative methods, *i.e.*, the trial-and-error method and the Evolutionary Algorithms (EA)-based methods[20,22,26,36], are usually used. A staged evolution is used to derive the parameters. Firstly, numerical simulation is used to analyze the effect of each parameter on the output signal and accelerates the preliminary parameters setting. Secondly, a NSGA-based approach is applied to evolve the CoM trajectory generator, which is based on a fixed foot trajectory. Thirdly, NSGA-based evolution method is used to evolve parameters of the foot trajectory generator[37]. Finally, during the irregular terrain walking evolution, by entraining several paths of sensory feedback, adaptive walking patterns can be realized.

(1) Parameters analyses of CPG model

The first stage aims to find the general relationships between parameters and the oscillatory outputs (the parameter analysis method can be found in our previous work[38,39]). The connection weights between oscillators are set as inhibitory relationship in order to get desired output phase relationships as shown in Fig. 2.

(2) GA-based CoM trajectory generation

The second stage uses GA to evolve the three oscillators' parameters to generate the CoM trajectory. Here, genomes are coded as array of neural oscillator model parameters. The mapping parameters are adjusted and set as constants based on the evolution results of the oscillators for CoM trajectory. The feedback term is set to zero during the parameter evolution process.

The distance fitness measure takes into account the straight-line walking distance along a pre-specified direction (in this case, the x-direction), the robot reaches in a fixed time. It is described as:

$$fitness_{\text{dis}} = \sqrt{\left(x_{\text{end}} - x_0\right)^2}, \tag{7}$$

where x_0 and x_{end} are the initial position of the robot on the ground and the position of the robot at the end of the simulation, respectively. This fitness function expresses the distance traveled in a straight line (in the x-direction) to go from the first position of the robot to its last position. This fitness function achieving minimum means that the robot travels both far and straight in the desired direction.

The other fitness measure is to guarantee the smoothness of the walking pattern. It is postulated that a walking pattern with only small amplitudes of body shaking can reflect to some extent the stability of the walking. This fitness measure is:

$$fitness_{\text{atti}} = 1 / \left(\left|\theta_{\text{pitch}} - \theta_{\text{pitch\_limit}}\right| + \left|\theta_{\text{roll}} - \theta_{\text{roll\_limit}}\right|\right), \tag{8}$$

where, θ_{pitch} and θ_{roll} are the attitude inclinations in sagittal plane (x-direction) and coronal plane (y-direction), respectively. Small excursions in the sagittal and coronal planes (set as $\theta_{\text{pitch\_limit}}$, $\theta_{\text{roll\_limit}}$), respectively, may actually improve the stability of the upright walking pattern, so only angular deviations in excess of those amounts result in a detrimental effect on fitness values.

(3) NSGA-based foot trajectory generation

NSGA-II[37] is applied in the third stage to realize the gait pattern evolution. Genomes are coded as array of oscillator model parameters ($T_{\text{r\_foot}}$, $T_{\text{a\_foot}}$, s_{0_foot}, $\beta_{\text{\_foot}}$, $w_{\text{fe\_foot}}$) and the mapping parameters (X_0, Z_0, A_x, A_z). In this stage, the distance fitness is also applied. The parameter evolution process is treated as a minimization problem and thus the reciprocal of the $fitness_{\text{dis}}$ is used. The second fitness measure guarantees the walking stability. During stable walking, it is required that the ZMP should keep inside in the boundary of the supporting region of the feet (or foot). The larger the stable index D_s (as shown in Eq. (6)) is, the higher the stability is. D_s is chosen as the third fitness measure as:

$$fitness_{\text{ZMP}} = 1 / D_s, \tag{9}$$

During evolution, two boundary constraints are added to ensure the generation of stable oscillation signals of the oscillatory network, as:[30]

$$\left.\begin{aligned} \beta &\geq w_{\text{fe}} - 1 \\ w_{\text{fe}} &> 1 + T_{\text{r}} / T_{\text{a}} \end{aligned}\right\}, \tag{10}$$

Finally, by entraining several paths of sensory feedback, adaptive walking patterns can be designed and realized. The feedback coefficients are obtained through simulations and experiments. During the exploration of the feedback coefficients, other parameters, including the model parameters and mapping parameters, are unchanged.

3 Simulations and experiments

3.1 Experiment platform

NAO is used as the hardware platform (Fig. 4). This robot is equipped with a variety of sensors including a 3-axis accelerometer and a 2-axis gyroscope. This work only considers the 10 DoFs on two legs (2 in the hip, 2 in the ankle and 1 at the knee); the position control signals of the HipYawPitch DoFs are set as fixed values.

In this work, the adaptive characteristics of the

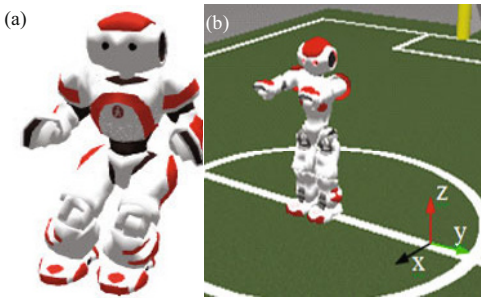

Fig. 4 Humanoid robot platform. (a) The NAO robot; (b) the ODE-based simulation environment.

workspace trajectories will be mapped to the joint space using the motion engine. The desired joint positions for the joints PD servos are obtained through inverse kinematics and are used to control the actuators[30]. The parameters evolution process is carried out under a physical simulation environment (Webots), as shown in Fig. 4b, and then dubbed to the real robot. The evolved parameters are realized on the simulated NAO robot. In this work, the servos control the joints to track the reference signals using built-in PD-type servo mechanism.

3.2 Walking pattern evolution

(1) CoM trajectory generator

The simulation is carried out using the ODE-based simulator with GA evolution. Two objective functions $fitness_{dis}$ and $fitness_{atti}$ are combined to evolve the CoM trajectory

$$fitness = \omega_1 \times fitness_{\text{dis}} + \omega_2 \times fitness_{\text{atti}}, \qquad (11)$$

where $\omega_1 > 0$, $\omega_2 > 0$ ($\omega_1 + \omega_2 = 1$) are weighting coefficients and can be adjusted according to request. The parameters of GA are set as: the population size: 50, the maximum generation: 60, the selection ratio: 0.5, the crossover ratio: 0.6 and the mutation ratio: 0.3.

At the start of the evolution, NAO only can walk a short distance and the fitness is low. After about 18 generations (Fig. 5), the robot can realize stable straight walking. Table 1 shows the parameters of the CoM trajectory generator. These parameters are set as constants in the following simulations, independent of the walking terrains.

(2) Foot trajectory generator

Deb's NSGA-II[36] is used to evolve the best parameters of the control system to realize flat terrain walking. Binary tournament selection, intermediate crossover and the Gaussian mutation methods are used in this study.

Often, the advised value of the crossover probability is relatively large (0.25 to 0.9) to ensure a good crossover rate. Crossover probability close to the upper limit will greatly increase the randomness of evolutionary algorithms due to their high possibilities of destructing the individuals with good genes. However, when the crossover probability is close to the lower limit, most individuals will be retained for the next generation, and as consequences, the diversity of the population and the convergence rate of the algorithm will be accordingly

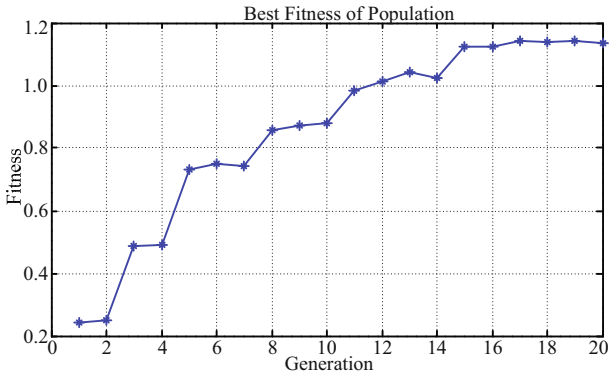

Fig. 5 The fitness changes in the process of evolution of the best individual.

Table 1 Parameters values of the CoM generator

Parameters	Values
T_{r_CoM}, T_{a_CoM}	0.1045, 0.345
s_{0_CoM}, $\beta_{\_\text{CoM}}$	0.611, 1.332
ω_{fe_CoM}, K_f	1.488, 0.06
K_x, off_x	0.009, 0.06
K_y, off_y	0.11, 0.0
K_z, off_z	0.012, 0.22

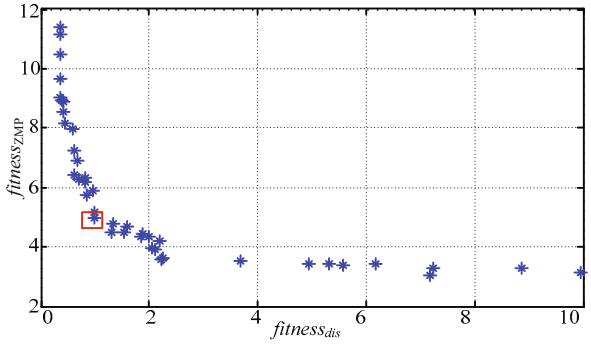

Fig. 6 Pareto front of generation 50.

Table 2 Values of the parameters

Parameters	Values
$T_{\text{r\_foot}}$, $T_{\text{a\_ foot}}$	0.117, 0.352
$s_{0\_\text{ foot}}$, $\beta_{\_\text{ foot}}$	0.576, 3.773
$\omega_{\text{fe\_ foot}}$	2.135
A_x, X_0	7.664, 4.023
A_z, Z_0	1.902, −0.001

decreased. Therefore, 0.75 is chosen for the interpolation crossover in the experiments. Mutation allows the random variation of individuals in the search space. The mutation probability also has an advised range (0.01 to 0.5). The larger the mutation probability is, the more stochastic the evolutionary algorithms are. A random search is expected if the mutation probability is ex-

tremely overlarge. On the other hand, with insufficient mutation, the variations of the individuals will be restrained to a very limited space, and fitter individuals will hence get less likely to be explored, leading to lower optimization efficiency. In the experiments, the mutation probability is set as 0.1.The generation size is set as 50 and the population size is selected as 50 individuals.

After about 35 generations, the robot can realize a stable straight walking pattern. The evolution results of the 50th generation are shown in Fig. 6, the tradeoff relationship between the two objectives is evident. One of the best solutions (marked in Fig. 6) is picked on the Pareto front, and Table 2 shows the parameters. These parameters of the neural oscillators are set as constants in the following experiments, independent of terrain.

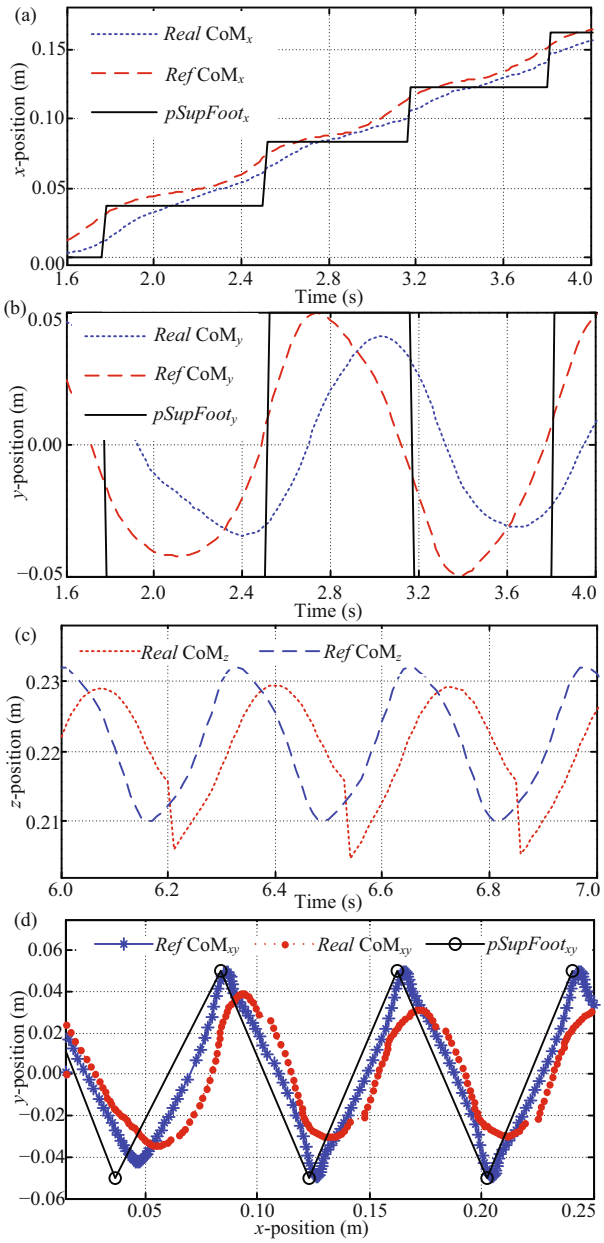

Fig. 7 The generated CoM trajectories. (a) CoM$_x$ trajectory; (b) CoM$_y$ trajectory; (c) CoM$_z$ trajectory; (d) CoM trajectory in x-y plane.

The biped flat terrain walking experiment is conducted about 40 seconds, and parts of the experiment results are shown from Fig. 7 to Fig. 9. In Fig. 7a, the red trajectory is the generated reference CoM$_x$, the blue trajectory is the real CoM$_x$ during NAO robot walking, which is calculated by the kinematics model based on the position measurement using the internal joint position sensor. The black trajectory pSupFoot$_x$ represents the position of the supporting foot in x-direction. The execution time of NAO is 20 ms frame. Figs.7 b and 7c are the generated CoM$_y$ and CoM$_z$ trajectories, independently. As Fig. 7 shows, there have certain phase differences between the reference and real CoM trajectories, which may be due to the control delay and the joint position sensor transmission delay.

Fig. 8 shows the generated foot trajectory. The ZMP (Fig. 9a) and body attitude information (Fig. 9b) are used to show the walking performance. As Fig. 9a shows, the foot boundary is about 0.04 m larger than the

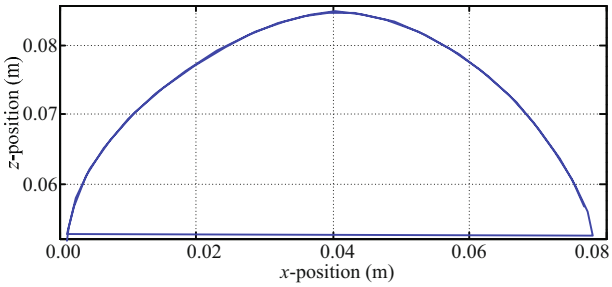

Fig. 8 The generated foot trajectory.

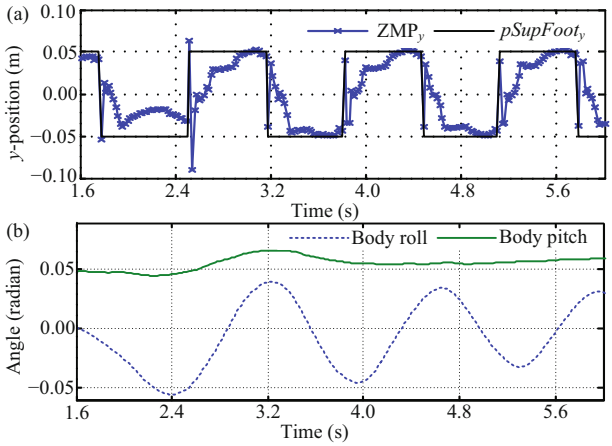

Fig. 9 ZMP distribution and the body attitude angles during the flat terrain walking. (a) ZMP distribution; (b) body attitude angles.

foot position, so the ZMP trajectories are within the upper and lower boundaries of foot trajectories.

3.3 Walking on inclined terrains

This study considers several terrain models, including up and down regular inclined planes, inclined planes with changing slope angles, terrain surfaces with distributed unknown bumps (for example, small height variations of a few centimeters or slope changes of a few degrees, ascending or descending stairs).

3.3.1 Regular slope-terrain adaptive walking

Inclined planes are typically encountered in human environments. The experimental environment is designed as three-staged terrains, including a flat surface, uphill and downhill segments (slopes up to 15˚). The transitions between the terrain segments can be considered to be perturbations. Without the prior knowledge of the walking terrain, in order to realize the adaptive walk, the body-attitude-based reflex method is used in this work. The body attitude θ can be estimated by using the gyroscope and accelerometer of the NAO robot. The designed calculation method is shown in Fig. 10, where θ_{acc} is the body attitude calculated by the accelerometer, and θ_{gyro} is the body attitude calculated by the gyroscope. A Low pass Filter (LF) and a High pass Filter (HF) are used to get the dynamic and static characteristics of θ_{acc} and θ_{gyro} .

(1) Feedback via CoM trajectory generator. The attitude information feedback to the neural oscillator corresponding to the CoM$_x$ trajectory is expressed as:

$$CoM_{x\_\text{feed}} = CoM_x - K_1\theta_{\text{pitch}}, \tag{12}$$

where K_1 is gain. The purpose of the feedback loop is to adjust the CoM_x along the slope surface to prevent slippage on up slope surface walking and overturning during down slope walking.

(2) Feedback via foot trajectory generator. The attitude information is coupled to the neural oscillators of the foot trajectory generator is expressed as:

$$feed_i^{\{\text{e,f}\}} = \mp K_2\theta_{\text{Pitch}}, \tag{13}$$

where K_2 is the gain. The purpose of the feedback design is to adjust the amplitude of the oscillatory outputs. Thus, gait patterns with adaptive step length and step height can be generated.

The slope-adaptive walking experiment was conducted about 70 seconds. Some of the results are shown in Figs. 11 and 12. Fig. 11a shows that the θ_{pitch} can represent the changes of body attitude on different walking terrains. Fig. 11b shows that entraining with the perceived θ_{pitch}, the position of the CoM$_x$ can be adjusted online, and that the swing foot trajectory with adaptive step length and step height can be realized. When walking up the slope, the position of the CoM$_x$ moves forward along the slope. In contrast, the CoM$_x$ is moved backward during down slope walking. Meanwhile, as shown in Fig. 11c, the adaptive foot trajectories during

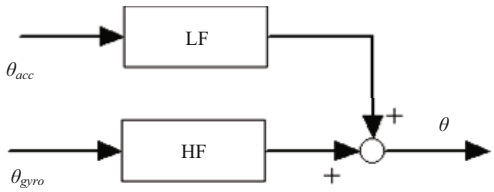

Fig. 10 Calculation of the body attitude angle.

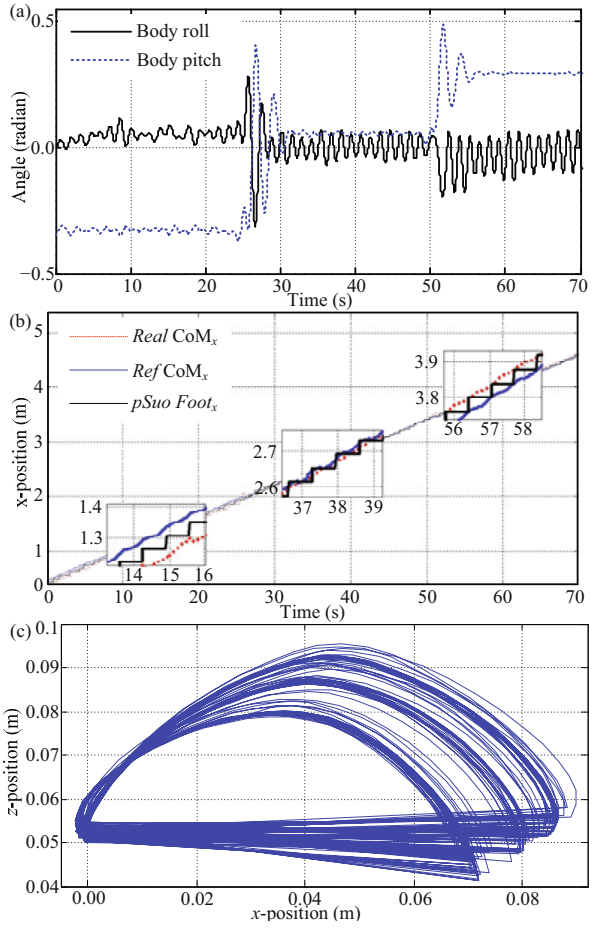

Fig. 11 The online generated CoM trajectory and foot trajectory. (a) The body attitude; (b) the generated CoM$_x$; (c) the generated swing foot trajectory in sagittal plane.

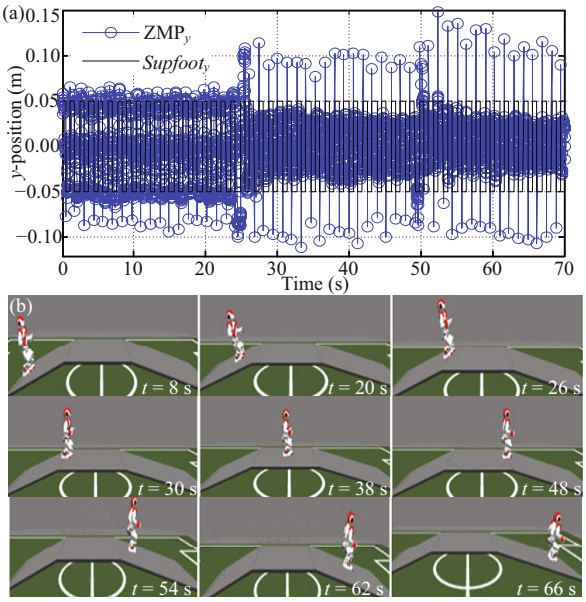

Fig. 12 Simulation of NAO walking on sloped terrain. (a) The distribution of ZMP; (b) screenshots of a successful walking pattern on sloped terrain (uphill 15˚, downhill 10˚).

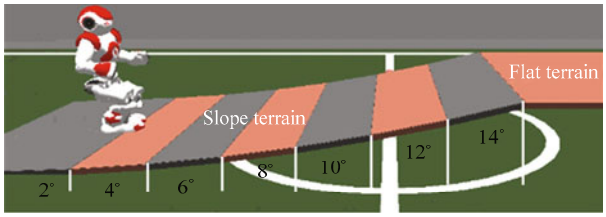

Fig. 13 The simulated changing slope-terrain.

sloped terrain walking can be generated online. The walking step length and step height can be adjusted according to the walking terrain.

While walking on sloped terrain both up and down, NAO can maintain stable and shows only a bit staggering during the transitions. As Fig. 12a shows, the ZMP remains within the foot support area of the robot except during the switching phase of the supporting leg, which reflects that stable walking performance can be achieved. Fig. 12b shows the snapshots of the adaptive walking simulation.

The simulation experimental results indicate that the control system is successful with a stable walk in the transition from a horizontal plane onto an inclined terrain.

3.3.2 Changing slope-terrain adaptive walking

In the second set of simulation experiments, the NAO robot walks in an inclined environment with varied slope angles as shown in Fig. 13.

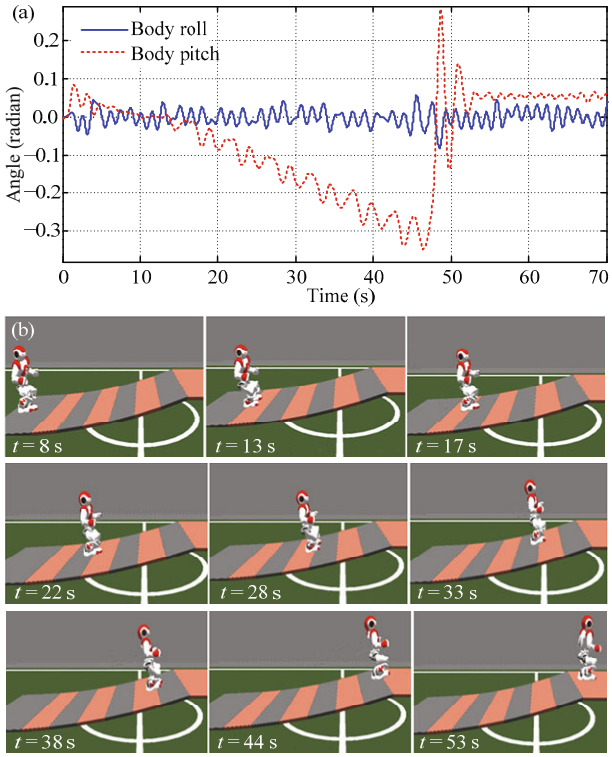

Fig. 14 Simulation of NAO walking on terrain with increasing slopes. (a) The body attitude in pitch and roll planes; (b) the screenshots of successful walking on terrain with increasing slopes.

Two feedback paths are used, as introduced in the experimental setup described above, to automatically modulate the generated trajectories online. Fig. 14a shows the body attitude changes and the snapshots of the walking are shown in Fig. 14b.

3.3.3 Stair-terrain adaptive walking

To further verify the superiority of the presented control strategy, experiments of adaptive biped walking were carried out on more irregular terrains. The walking terrain was set up with bumps of 0.8 cm in height and stairs of 2.0 cm in height. The ZMP feedback and body attitude feedback paths were combined to realize the generation of the adaptive CoM trajectories and swing foot trajectories.

(1) Feedback via CoM trajectory generator. The feedback information is coupled to the neural oscillators, corresponding to CoM$_x$ and CoM$_z$ are expressed as:

$$CoM_{x\_\text{feed}} = CoM_x - K_3 \times \theta_{\text{pitch}}, \quad (14)$$

$$CoM_{z\_\text{feed}} = CoM_z + K_4 \times D_s, \quad (15)$$

where K_3 and K_4 are feedback gain coefficients. The

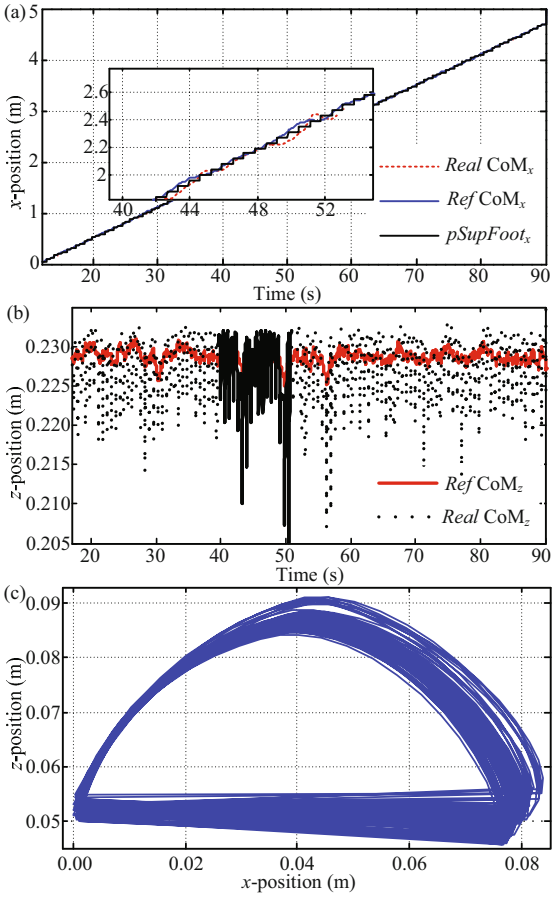

Fig. 15 Simulation results1: the generated CoM trajectory and foot trajectory. (a) The generated CoM$_x$ trajectory; (b) the generated CoMz trajectory; (c) the generated foot trajectory.

purpose is to use the feedback information to adjust the CoM$_x$ along the sloped terrain and adjust the height of the CoM$_z$ to prevent of slippage and overturning during the sloped terrain walking.

(2) Feedback via foot trajectory generator. The feedback information is coupled to the oscillator network, and is expressed as:

$$feed_i^{\{e,f\}} = \pm K_5 \times D_s, \tag{16}$$

where K_5 is the gain coefficient. This purpose is to use the stability information to adjust the amplitude of the output signals. Thus, the gait pattern with adaptive step length and height can be generated.

Figs. 15 and 16 show some of the results. When the acceleration sensor and gyro sensor detect the inclination in the pitch plane, the CoM in the *x*-direction is adjusted online as shown in Fig. 15a. When the FSR sensors detect the ZMP outside the stable range, the CoM in the *z*-direction (Fig. 15b) and the gait patterns (Fig. 15c) are adjusted in real time to realize adaptive walking.

Fig. 16a shows the distribution of the ZMP during walking on irregular terrain. The ZMP almost keeps within the support area of foot except near the walking terrain transition points. Some of the snapshots of the experimental simulation are shown in Fig. 16b.

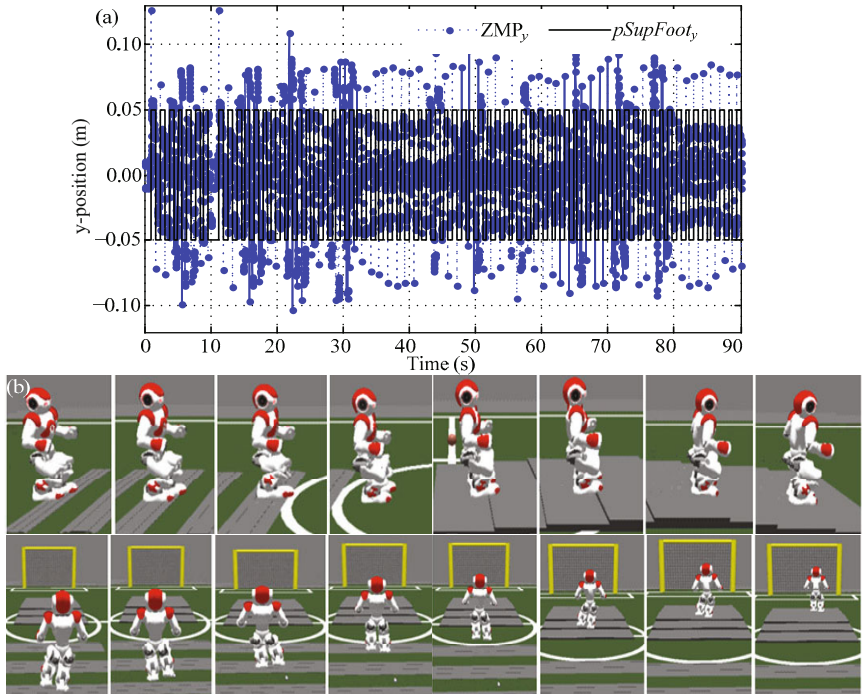

Fig. 16 Simulation results 2: walking on stair-terrain. (a) The distribution of ZMP during irregular terrain walking; (b) snapshots of the simulation experiment.

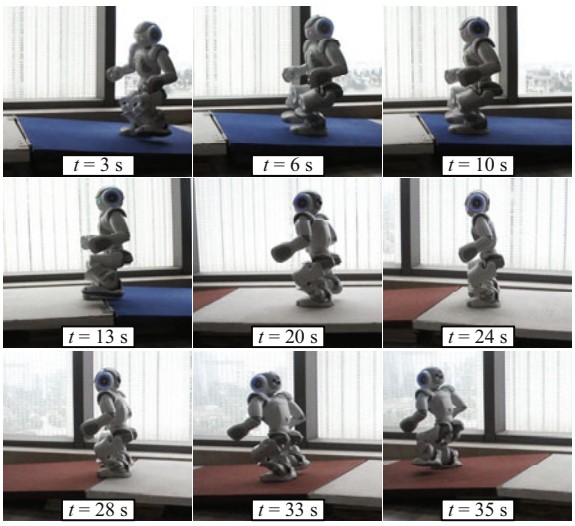

Fig. 17 Real NAO robot biped sloped terrain adaptive walking experiment.

3.4 Inclined terrain adaptive walking experiment

The simulated typical walking terrain adaptive walking verified the feasibility of the presented control strategy. Based on the Webots simulation results, the program was dubbed to the real NAO to test its walking performance. In this work, since ODE cannot provide precise dynamical modelling and the friction force differences between the simulation and real walking terrains, the gains of the feedback loops need to be modulated by trial and error within a very small range.

One experiment was set up to test the robot performance without prior knowledge of the terrains. The experiment allowed the robot to walk over three stages of an inclined terrain (inclined surfaces with about 6° slopes) and the connected stage was a flat terrain. The walking surface was an elastic deformable platform, and the friction coefficient between the feet and the walking surface was not large enough to avoid slippage. Every step of NAO on the platform could cause the walking surface to deform and slippage could occur. During the inclined terrain walking, the body-attitude-based feedback paths were used to adjust the generated CoM and foot trajectories automatically. Parts of experiment snapshots are shown in Fig. 17. By entraining the feedback information, the basic walking pattern evolved by the EA was adjusted automatically, so the robot adapted to the terrain conditions autonomously.

The differences between Webots simulations and experiments are due to the measurement noise, offset, and robot model uncertainties, including joint compliance and the slip between the feet of NAO and the walking surface. NAO robot only showed a bit of staggering during the terrain transitions. The experiments show that the generated trajectories are applicable and workable.

4 Conclusion

This work uses the dynamic properties of neural oscillators to develop an online trajectory generation method. In this work, by using two set of neural oscillators, adjustable workspace trajectories can be generated online. The proposed control strategy allows a biped robot to overcome the limitations of the conventional biped walking control methods. In this method, the neural oscillators are allocated in the workspace space to generate trajectories, so the robot can simplify the design of connection weights and feedback pathways. Moreover, by entraining two or more feedback loops to prevent slippage and overturning, it can negotiate steeper slopes than the conventional control method.

Acknowledgment

This work is supported by National Natural Science Foundation (Nos. 61673300, 61573260) and Fundamental Research Funds for the Central Universities, and Natural Science Foundation of Shanghai (No.16JC1401200).

References

[1] Shih C L. Ascending and descending stairs for a biped robot. *IEEE Transactions on Systems*, *Man*, *and Cybernetics - Part A*: *System and Humans*, 1999, **29**, 255–268.

[2] Huang Q, Yokoi K, Kajita S, Kaneko K, Arai H, Koyachi N, Tanie K. Planning walking patterns for a biped robot. *IEEE Transactions on Robotics and Automation*, 2001, **17**, 280–289.

[3] Sugihara T, Nakamura Y, Inoue H. Real time humanoid motion generation through ZMP manipulation based on inverted pendulum control. *Proceeding of the International Conference on Robotics and Automation*, Washington, USA, 2002, **2**, 1404–1409.

[4] Kajita S, Kanehiro F, Yokoi K, Hirukawa H. The 3D linear inverted pendulum mode: A simple modeling for a biped walking pattern generation. *Proceeding of the International Conference on Intelligent Robots and Systems*, Maui, USA, 2001, **1**, 239–246.

[5] Park I W, Kim J Y, Lee J, Oh J H. Online free walking

trajectory generation for biped humanoid robot KHR-3 (HUBO). *Proceeding of the International Conference on Robotics and Automation*, Orlando, Florida, USA, 2006, 1231–1236.

[6] Seven U, Akbas T, Fidan K C, Erbatur K. Bipedal robot walking control on inclined planes by fuzzy reference trajectory modification. *Soft Computing*, 2012, **16**, 1959–1976.

[7] Li T, Ceccarelli M, Luo M Z, Laribi M A, Zeghloul S. An experimental analysis of overcoming obstacle in human walking. *Journal of Bionic Engineering*, 2014, **11**, 497–505.

[8] Brown T G. On the nature of the fundamental activity of the nervous centres; together with an analysis of the conditioning of rhythmic activity in progression, and a theory of the evolution of function in the nervous system. *The Journal of Physiology*, 1914, **48**, 18–46.

[9] Grillner S. Neural control of vertebrate locomotion — central mechanisms and reflex interaction with special reference to the cat. In: Barnes W J P, Gladden M H, eds., *Feedback and Motor Control in Invertebrates and Vertebrates*, Springer Netherlands, London, UK, 1985, 35–56.

[10] Chiang M H, Chiang F R. Anthropomorphic design of the human-like walking robot. *Journal of Bionic Engineering*, 2013, **10**, 186–193.

[11] Ren L, Qian Z H, Ren L Q. Biomechanics of musculoskeletal system and its biomimetic implications: A review. *Journal of Bionic Engineering*, 2014, **11**, 159–175.

[12] Ijspeert A J. Central pattern generators for locomotion control in animals and robots: A review. *Neural Networks*, 2008, **21**, 642–653.

[13] Wu Q D, Liu C J, Zhang J Q, Chen Q J. Survey of locomotion control of legged robots inspired by biological concept. *Science in China Series F*: *Information Sciences*, 2009, **52**, 1715–1729.

[14] Yu J Z, Tan M, Chen J, Zhang J. A survey on CPG-inspired control models and system implementation. *IEEE Transactions on Neural Networks and Learning Systems*, 2014, **25**, 441–456.

[15] Li C, Lowe R, Ziemke T. A novel approach to locomotion learning: Actor-critic architecture using central pattern generators and dynamic motor primitives. *Frontiers in Neurorobotics*, 2014, **8**, 1–17.

[16] Ijspeert A J, Crespi A, Ryczko D. From swimming to walking with a salamander robot driven by a spinal cord model. *Science*, 2007, **315**, 1416–1420.

[17] Yu J, Ding R, Yang Q, Tan M, Wang W, Zhang J. On a bio-inspired amphibious robot capable of multimodal motion. *IEEE*/*ASME Transactions on Mechatronics*, 2012, **17**, 847–856.

[18] Santos C P, Matos V. CPG modulation for navigation and omnidirectional quadruped locomotion. *Robotics and Autonomous Systems*, 2012, **60**, 912–927.

[19] Fukuoka Y, Kimura H. Dynamic locomotion of a biomorphic quadruped "Tekken" robot using various gaits: Walk, trot, free-gait and bound. *Applied Bionics and Biomechanics*, 2009, **6**, 1–9.

[20] Park C S, Hong Y D, Kim J H. Evolutionary-optimized central pattern generator for stable modifiable bipedal walking. *IEEE*/*ASME Transactions on Mechatronics*, 2014, **19**, 1374–1383.

[21] Or J. A hybrid CPG-ZMP controller for the real-time balance of a simulated flexible spine humanoid robot. *IEEE Transaction on System*, *Man*, *and Cybernetics - Part C*: *Application and Reviews*, 2009, **39**, 547–561.

[22] Hong Y. D, Park C S, Kim J H. Stable bipedal walking with a vertical center-of-mass motion by an evolutionary optimized central pattern generator. *IEEE Transactions on Industrial Electronics*, 2014, **61**, 2346–2355.

[23] Nassour J, Henaff P, Benouezdou F. Multi-layered multi-pattern CPG for adaptive locomotion of humanoid robots. *Biological Cybernetics*, 2014, **108**, 291–303.

[24] Taga G. Self-organized control of bipedal locomotion by neural oscillators in unpredictable environment. *Biological Cybernetics*, 1991, **65**, 147–159.

[25] Taga G. A model of the neuro-musculo-skeletal system for human locomotion. *Biological Cybernetics*, 1995, **73**, 97–121.

[26] Endo G, Morimoto J, Matsubara T, Nakanishi J, Cheng G. Learning CPG-based biped locomotion with a policy gradient method: Application to a humanoid robot. *International Journal of Robotics Research*, 2008, **27**, 213–228.

[27] Ha I, Tamura Y, Asama H. Gait pattern generation and stabilization for humanoid robot based on coupled oscillators. *Proceeding of the International Conference on Intelligent Robots and Systems* (*IROS*), San Francisco, USA, 2011, **10**, 3207–3212.

[28] Aoi S, Tsuchiya K. Locomotion control of a biped robot using nonlinear oscillators. *Autonomous Robots*, 2005, **19**, 219–232.

[29] Liu C J, Wang D W, Chen Q J. Central pattern generator inspired control for adaptive walking of biped robots. *IEEE Transactions on Systems*, *Man*, *and Cybernetics - Part A*: *Systems and Humans*. 2013, **43**, 1206–1215.

[30] Kajita S, Hirukawa H, Yokoi K, Harada K. *Humanoid Robots*, Ohm-sha, Ltd., Tokyo. Japanese, 2005. (in Japanese)

[31] Matsuoka K. Sustained oscillations generated by mutually inhibiting neurons with adaptation. *Biological Cybernetics*,

1985, **52**, 367–376.

[32] Amrollah E, Henaff P. On the role of sensory feedbacks in rowat selverston CPG to improve robot legged locomotion. *Frontiers Neurorobot*, 2010, **4**, 1–9.

[33] Righetti L, Ijspeert A J. Programmable central pattern generators: An application to biped locomotion control. *Proceeding of the International Conference on Robotics and Automation* (*ICRA*), Orlando, USA, 2006, 1585–1590.

[34] Li G, Zhang H, Zhang J, Bye R T. Development of adaptive locomotion of a caterpillar-like robot based on a sensory feedback CPG model. *Advanced Robotics*, 2014, **28**, 389–401.

[35] Fukuoka Y, Habu Y, Fukui T. Analysis of the gait generation principle by a simulated quadruped model with a CPG incorporating vestibular modulation. *Biological Cybernetics*, 2013, **107**, 695–710.

[36] Oliveira M, Matos V, Santos C P, Costa L. Multi-objective parameter CPG optimization for gait generation of a biped robot. *Proceeding of the International Conference on Robotics and Automation* (*ICRA*), Karlsruhe, Germany, 2013, 3130–3135.

[37] Deb K, Pratap A, Agarwal S, Meyarivan T. A fast and elitist multi-objective genetic algorithm: NSGA-II. *IEEE Transaction on Evolutionary Computation*, 2002, **6**, 181–197.

[38] Liu C J, Seo K, Fan Z, Tan X B, Goodman E D. Synthesis of Matsuoka-based neuron oscillator models in locomotion control of robots. *Global Congress on Intelligent Systems*, Wuhan, China, 2012, **42**, 342–347.

[39] Liu C J, Chen Q J, Wang D W. CPG-inspired workspace trajectory generation and adaptive locomotion control for quadruped robots. *IEEE Transactions on Systems*, *Man*, *and Cybernetics-Part B*: *Cybernetics*, 2011, **41**, 867–880.